

Shell masers

Moshe Elitzur¹ and Valentín Bujarrabal²

¹ Department of Physics and Astronomy, University of Kentucky, Lexington, KY 40506, USA; moshe@pa.uky.edu

² Centro Astronómico de Yebes (IGN), Apartado 148, 19080 Guadalajara, Spain; bujarrabal@cay.es

Received April 25, 1995; accepted August 3, 1995

Abstract. We present the analytical solution of a maser shaped like a spherical shell. We determine the general condition on the size of the central cavity at which a sphere becomes a shell maser, and derive the intensity, beaming angle and observed size of both unsaturated and saturated shells.

Key words: Masers – Radiative Transfer – Circumstellar Matter

1. Introduction

Given a pumping scheme, the brightness temperature of an unsaturated maser can be immediately determined from the source's length along the line of sight because the gain, τ , is simply proportional to it; there is no need to even consider the geometrical shape. In a saturated maser, on the other hand, the dependence of gain on distance traveled through the source varies between the saturated and unsaturated domains. As a result, the brightness temperature in any given direction cannot be determined before a complete solution of the full maser structure has been attained. An analytic solution of this highly non-linear problem is possible because, in all sources with an appreciable gain, maser radiation is highly beamed (e.g. Elitzur 1990b; hereafter E90): at any location in an arbitrarily shaped maser, the longest chord through the source provides the direction of the local dominant ray and maser radiation is mostly confined to a small beam around it. The complete, detailed solution is highly dependent on the source geometry; indeed, it cannot even be attempted without fully specifying the geometry. Thus far, detailed solutions have been derived for linear masers (Elitzur 1990a), for the planar geometry of a disk (Elitzur et al. 1992), and for the three dimensional configurations of spheres and filaments (Goldreich & Keeley 1972, E90, Elitzur et al. 1991).

Send offprint requests to: V. Bujarrabal

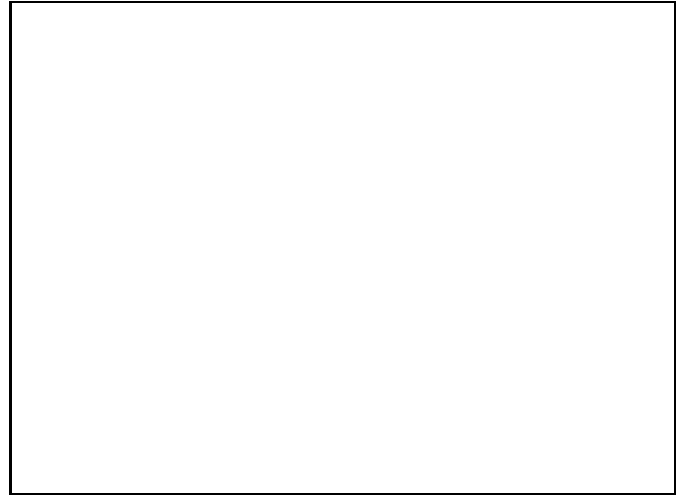


Fig. 1. Geometrical notations for a shell maser.

Recent interferometric observations of masers in late-type stars reveal ring-like structures, indicative of a shell geometry. The observations include both H₂O (Reid & Menten 1990) and SiO (Diamond et al. 1994, Miyoshi et al. 1994, Greenhill et al. 1995). The shell geometry is fundamentally different from all the maser geometries considered until now, which will be referred to as “regular”. In regular geometries there is a single dominant ray at virtually every point (the only exception is an occasional singularity, such as the center of a sphere or a disk maser). The dominant ray is aligned with the local axis of symmetry and its direction coincides with that of the flux vector. In contrast, at an arbitrary point in a shell there are many chords of maximal length belonging to the rays that graze the core (see Fig. 1). Thus the dominant rays in a shell maser span the surface of a cone whose axis is aligned with the radius vector. From symmetry, the flux vector points in the direction of that axis and it does not coincide with the direction of any dominant ray.

Maser emission from shells has been studied thus far only in numerical calculations (Western & Watson 1983;

Bujarrabal 1994). Utilizing the techniques developed in the studies of regular geometries, we present here the complete analytical solution of shell masers. Since the solution methods are described in detail in the referenced literature, the presentation here centers mostly on the features unique to the shell geometry.

2. Generalities

Consider a maser shaped as a spherical shell with inner radius R_i and outer radius R (Fig. 1). As in all previous solutions, the shell is assumed uniform and quiescent (no ordered motions). At a point in the shell characterized by radius r , the longest chords belong to the rays that graze the core, inclined at $\theta_0 = \sin^{-1}(R_i/r)$ to the radius vector. Introduce dimensionless variables x and x_i such that

$$r = xR, \quad R_i = x_iR, \quad \theta_0 = \sin^{-1}(x_i/x). \quad (1)$$

That is, x_i is the relative size of the cavity, and positions in the shell are characterized by $x_i \leq x \leq 1$.

Denote the intensity along a dominant ray of any maser I_0 . In regular geometries the radiation is confined mostly to $|\theta| \leq \theta_b$, where θ is measured from the local symmetry axis and θ_b ($\ll 1$) is the beaming angle. Therefore, the angle-averaged intensity is $J \simeq \frac{1}{4}I_0\theta_b^2$, if the intensity is assumed approximately constant inside the maser beam. In shell masers, on the other hand, the radiation is confined mostly to $\theta_0 \leq \theta \leq \theta_0 + \theta_b$ (see Sec. 3 below). Neglecting rays outside the main beam, the angle-averaged intensity for a constant intensity inside the beam is

$$J = \frac{1}{2} \int I \sin \theta d\theta \simeq \frac{1}{2}I_0\theta_b \left(\sin \theta_0 + \frac{1}{2}\theta_b \cos \theta_0 \right). \quad (2)$$

Instead of a rectangular intensity profile we can employ an exponential fall-off, $I \propto \exp[-(\theta - \theta_0)/\theta_b]$. This angular distribution produces the same result except that the factor $\frac{1}{2}$ inside the parentheses is replaced by unity.

When $\theta_0 \ll \frac{1}{2}\theta_b$ ($\ll 1$), the second term in the parentheses dominates and the result of regular geometries is recovered. Therefore, the shell is properly described by the spherical maser solution as long as its central cavity is sufficiently small that $\theta_0 < \frac{1}{2}\theta_b$. The shell structure must be considered only in the reverse situation in which the first term in the parentheses dominates and the spherical solution no longer applies. So the transition to a shell maser occurs when

$$\theta_0 > \theta_b, \quad (3)$$

omitting the factor $\frac{1}{2}$ to accommodate also the exponential profile. This condition, similar to the filamentary condition that defines elongated masers (Elitzur et al. 1991), will be referred to as the *shell condition*. At the inner surface ($x = x_i$), $\theta_0 = \pi/2$ and the condition is trivially obeyed. It provides the most meaningful constraint at the outer surface ($x = 1$), where θ_0 is minimal.

The meaning of the shell condition is quite simple. On the surface of a spherical maser, the radiation fills a cone with an opening angle θ_b centered on the radius vector. Now begin to carve a hole at the center of the sphere. As long as that hole is contained in the radiation cone it can be ignored and the maser remains a sphere. The maser becomes a shell once the hole emerges from the side of the radiation cone, i.e., when the shell condition is obeyed. The angle-averaged intensity in a shell maser is thus

$$J = \frac{1}{2}I_0\theta_b \sin \theta_0 = \frac{1}{2}I_0\theta_b \frac{x_i}{x}. \quad (4)$$

To a distant observer, the maser appears as a ring-like structure with inner radius R_i and outer radius $R_i + H$, where

$$H = R\theta_b \sqrt{1 - x_i^2} \quad (5)$$

and θ_b is the beaming angle at the surface. Observations can directly determine only the inner radius R_i and the thickness H . The outer radius R is unobservable, thus the ratio x_i cannot be directly determined. This problem exists of course in all regular geometries, too, where the only maser dimension amenable to observations is the observed size in the plane of the sky, not the length along the line of sight. Neither the radius of a spherical maser nor the length of a filamentary maser nor the length along the line of sight of a planar maser are directly observable (e.g. Elitzur et al. 1992).

Consider now the maser flux. In regular geometries the flux vector points in the direction of the dominant ray and is dominated by the contribution of $\theta = 0$, thus its magnitude obeys $F \simeq 4\pi J$. In a shell maser, on the other hand, the directions of the dominant ray and flux vector are different. Since the flux is dominated by the contribution of $\theta = \theta_0$, its magnitude obeys

$$\begin{aligned} F &= \int \cos \theta I d\Omega \simeq \cos \theta_0 \int I d\Omega \\ &= \cos \theta_0 \times 4\pi J = 4\pi J \sqrt{1 - (x_i/x)^2}. \end{aligned} \quad (6)$$

The result for regular geometries is recovered when $x_i = 0$. The flux vanishes on the shell's inner surface because non-dominant rays were neglected.

3. Unsaturated shell masers

The optical depth in an unsaturated maser is always proportional to pathlength. At an arbitrary position in the shell, denote the length of the longest chord ℓ_0 . A ray inclined to this chord at a small angle $\delta\theta$ (> 0) has a length

$$\begin{aligned} \ell &= r \cos(\theta_0 + \delta\theta) + \sqrt{R^2 - r^2 \sin^2(\theta_0 + \delta\theta)} \\ &\simeq \ell_0 - \ell_1 \delta\theta - \ell_2 \delta\theta^2, \end{aligned} \quad (7)$$

where

$$\begin{aligned}\ell_0 &= R \left(\sqrt{x^2 - x_i^2} + \sqrt{1 - x_i^2} \right) \\ \ell_1 &= R_i \left(1 + \sqrt{\frac{x^2 - x_i^2}{1 - x_i^2}} \right) \\ \ell_2 &= \frac{1}{2}R \left[\sqrt{x^2 - x_i^2} + \frac{x^2 - 2x_i^2 + x_i^4}{(1 - x_i^2)^{3/2}} \right].\end{aligned}\quad (8)$$

In regular geometries the dominant ray corresponds to a true maximum of the geometrical surface, i.e., $d\ell/d\theta = 0$ and the variation of ℓ with $\delta\theta$ is quadratic. In a shell the dominant ray does not correspond to a true maximum, the first derivative does not vanish and the variation of ℓ with $\delta\theta$ includes a linear term (which properly vanishes when $R_i = 0$). As a result, the angular distribution in an unsaturated shell is

$$I(\delta\theta) = I_0 e^{-\kappa_0 \ell_1 \delta\theta - \kappa_0 \ell_2 \delta\theta^2}. \quad (9)$$

Here κ_0 is the unsaturated absorption coefficient¹ and $I_0 = S \exp(\kappa_0 \ell_0)$, where S is the source function. The intensity detected by an external observer is obtained by substituting $x = 1$, which produces $\ell_0 = 2\ell_2 = 2R\sqrt{1 - x_i^2}$ and $\ell_1 = 2R_i$. Instead of the standard Gaussian that typifies the angular distribution of spherical maser radiation, the argument of the exponential contains a term linear in $\delta\theta$. At very small $\delta\theta$ the linear term dominates, at very large $\delta\theta$ the quadratic term. The shell condition ensures that the linear term dominates inside the entire maser beam, $\delta\theta \leq \theta_b$. With the dominance of this term, the radiation at any point in an unsaturated shell maser varies with direction in proportion to $\exp(-\delta\theta/\theta_b)$, where

$$\theta_b = \frac{1}{\kappa_0 \ell_1} \quad (10)$$

is the beaming angle. At the shell's outer surface $\theta_b = 1/(2\kappa_0 R_i)$, and the shell condition becomes

$$x_i^2 > \frac{1}{\kappa_0 R}. \quad (11)$$

A factor of $\frac{1}{2}$ was omitted on the right-hand side to provide a slightly more stringent constraint, in line with another estimate described below.

Only rays with $\delta\theta > 0$ were considered thus far. Rays with $\delta\theta < 0$ cut through the cavity and the decrease in their length from ℓ_0 is dominated by a term proportional to $\sqrt{-\delta\theta}$, much steeper than the linear decline for $\delta\theta > 0$. For all practical purposes, the angular distribution can always be assumed to have a sharp cutoff so that only $\theta \geq \theta_0$ need be considered.

¹ Following what is by now a standard procedure, the negative of the absorption coefficient is used for the maser transition so that it is positive.

The condition just derived was determined for unsaturated shells. However, a maser cannot become saturated unless it was first unsaturated and had to obey this condition during its unsaturated phase to be considered a shell. Therefore, Eq. 11 is the general condition that must be obeyed by all shell masers. For saturated shells we have to consider the magnitude of $\kappa_0 R$ that the maser must have had to become saturated. Typically, saturation occurs at $\kappa_0 R \gtrsim 10$, thus astronomical masers obey the shell condition when $x_i \gtrsim 0.3$.

General results for arbitrary x_i , displaying explicitly the transition from a sphere to a shell, can be obtained from the full angular distribution of Eq. 9. The requirement that the intensity drop to $1/e$ of its peak value produces a quadratic equation for the beaming angle whose solution is

$$\theta_b = \frac{\ell_1}{2\ell_2} \left(\sqrt{1 + z^{-2}} - 1 \right), \quad (12)$$

where $z = \kappa_0 \ell_1 / (2\sqrt{\kappa_0 \ell_2})$. When $z \gg 1$, equivalent to the shell condition of Eq. 11, the beaming angle of Eq. 10 is recovered. The opposite limit, $z \rightarrow 0$, properly reproduces the beaming angle of an unsaturated sphere, $\theta_b = 1/\sqrt{\kappa_0 R}$. Furthermore, the complete expression for J can be calculated from an integration of the full angular distribution, and the result is

$$J = \frac{1}{4} I_0 \frac{1}{\kappa_0 \ell_2} \left[1 - \sqrt{\pi} (z - \theta_0 \sqrt{\kappa_0 \ell_2}) e^{z^2} \operatorname{erfc} z \right]. \quad (13)$$

Again, utilizing properties of the error function erfc at large and small z reproduces the proper expressions for J in the respective limits.

From Eq. 5, the observed thickness of the maser ring obeys

$$\kappa_0 H = \frac{\sqrt{1 - x_i^2}}{2x_i}. \quad (14)$$

This result can also be obtained by noting that the surface brightness observed at infinity varies as $e^{-h/H}$, where h is the parallel linear displacement from the brightest ray. It is interesting that the observed thickness of unsaturated shells is independent of size,² the shell dimensions enter only in the ratio R_i/R .

Since the thickness H was derived assuming the shell condition, it diverges when $x_i \rightarrow 0$. Employing the full expression for the beaming angle, Eq. 12, removes the divergence and properly produces $H = \sqrt{R/\kappa_0}$ when $x_i = 0$, the observed size of an unsaturated spherical maser. In addition, the area generally provides a useful indicator for the effects of geometry on dimensions of the observed maser (see table 1 in Elitzur et al. 1992). The observed

² The maser size enters only indirectly through the condition $\kappa_0 R \gg 1$, required to ensure that the maser provides amplification sufficient to cause beaming.

area of an unsaturated shell maser, where $A_{\text{obs}} = 2\pi R_i H$, is

$$A_{\text{obs}} = \frac{\pi \ell_0}{2\kappa_0}, \quad (15)$$

where ℓ_0 is the longest chord at the outer surface. By comparison, in an unsaturated sphere, where $\ell_0 = 2R$ and the observed region is a small cap, $A_{\text{obs}} = 2\pi \ell_0 / \kappa_0$. Apart from a factor of 4, the expressions for the observed areas are the same.

4. Saturated shell masers

Consider now a sequence of masers with a fixed x_i , increasing $\kappa_0 R$. If the original maser obeys the shell condition, Eq. 11, subsequent masers obey it with a larger margin. The emerging intensity grows exponentially with maser size and at a certain radius, R_s , it obeys $J(x=1) = J_s$, i.e., the shell saturates. The corresponding radius obeys

$$\frac{1}{\kappa_0 R_s} \exp\left(2\kappa_0 R_s \sqrt{1-x_i^2}\right) = 4\gamma, \quad (16)$$

where $\gamma = J_s/S$; typically, astronomical masers have $\gamma \sim 10^5 - 10^7$. The approximate solution of this equation is

$$\kappa_0 R_s \simeq \frac{1}{2\sqrt{1-x_i^2}} \ln\left(\frac{2\gamma}{\sqrt{1-x_i^2}}\right), \quad (17)$$

a solution valid when the argument of the logarithm on the right-hand-side is large (e.g. E90). When $x_i = 0$, this result reproduces the saturation radius of a spherical maser.

With further increase in radius, the shell develops a two-zone structure: the inner zone, $R_i \leq r \leq r_s$, is unsaturated and has $\kappa \simeq \kappa_0$, the outer zone, $r_s \leq r \leq R$, is saturated and has $\kappa \simeq \kappa_0 J_s/J$. The boundary radius, $r_s \equiv x_s R$, is still unspecified. It is R_s for a maser that has just saturated and should shrink logarithmically as R increases.

4.1. The saturated shell

From Eq. 6, the flux divergence relation in a shell maser is

$$\frac{d}{dx} \left(x \sqrt{x^2 - x_i^2} J \right) = \kappa J R x^2. \quad (18)$$

Since in the saturated shell $\kappa J \simeq \kappa_0 J_s$, the solution there is immediate:

$$x \sqrt{x^2 - x_i^2} J - x_s \sqrt{x_s^2 - x_i^2} J_s = \frac{1}{3} J_s \kappa_0 R (x^3 - x_s^3). \quad (19)$$

Note that when $x \gg x_s$, $J = \frac{1}{3} J_s \kappa_0 r$, same as the result for a sphere (E90).

Along a ray that grazes the core, $I = I_0$ and $d\ell = d\ell_0$. Thus the radiative transfer equation past the mid-point of this path is

$$\sqrt{1 - \frac{x_i^2}{x^2}} \frac{dI_0}{dx} = \kappa R I_0. \quad (20)$$

With the aid of Eq. 4, the transfer equations for J and I_0 produce an equation for the beaming angle

$$\frac{d \ln(\theta_b x_i/x)}{dx} = -\frac{2x^2 - x_i^2}{x(x^2 - x_i^2)}. \quad (21)$$

The solution is straightforward, the result is

$$\theta_b = \theta_s \sqrt{\frac{x_s^2 - x_i^2}{x^2 - x_i^2}}, \quad (22)$$

where θ_s is the beaming angle at $x = x_s$; again, $x_i = 0$ reproduces the expression valid in the saturated zone of a spherical maser (E90). The angle θ_s can be obtained from the result for an unsaturated maser (Eq. 10), yielding

$$\theta_s = \frac{1}{\kappa_0 R x_i} \frac{\sqrt{1-x_i^2}}{\sqrt{1-x_i^2} + \sqrt{x_s^2 - x_i^2}} \simeq \frac{1}{\kappa_0 R_i}. \quad (23)$$

In the last relation we assumed that the thickness of the saturated zone greatly exceeds that of the unsaturated region, i.e., $1 - x_i \gg x_s - x_i$, an assumption justified for strongly saturated shells. The thickness of the observed maser ring is

$$H = \theta_s \sqrt{r_s^2 - R_i^2} \quad (24)$$

and its area is

$$A_{\text{obs}} = \frac{2\pi}{\kappa_0} \sqrt{r_s^2 - R_i^2}. \quad (25)$$

By comparison, the observed area of a saturated sphere is $\pi r_s / \kappa_0$.

The final quantity needed to complete the solution is r_s , the radius of the boundary between the saturated and unsaturated zones. It can be obtained from the requirement that, amplification by the unsaturated shell brings the intensity of the subordinate ray at core entrance to the dominant ray corresponding to J_s upon exit. The detailed steps are described in E90 and will be omitted here. The final result is controlled by the parameter

$$b = \ln\left(\frac{12\gamma x_i^2}{(\kappa_0 R)^2 \sqrt{1-x_i^2}}\right). \quad (26)$$

When the argument of the logarithm is much larger than unity, which is usually the case in astronomical masers, the boundary of the unsaturated zone obeys

$$(\kappa_0 r_s)^2 \simeq (\kappa_0 R_i)^2 + \frac{1}{4} b^2. \quad (27)$$

This enables us to complete the solution for a saturated shell maser. The beaming angle of the emergent radiation is

$$\theta_b = \frac{b}{2(\kappa_0 R)^2 x_i \sqrt{1 - x_i^2}}, \quad (28)$$

its intensity is

$$I_0 = \frac{4}{3b} J_s(\kappa_0 R)^3 \sqrt{1 - x_i^2} \quad (29)$$

and the thickness of the observed maser ring obeys

$$\kappa_0 H = \frac{b}{2\kappa_0 R_i}. \quad (30)$$

4.2. Complete saturation

As $\kappa_0 R$ increases while x_i is held fixed, the parameter b decreases logarithmically and $r_s \rightarrow R_i$ (see Eqs. 26 and 27); that is, the size of the unsaturated zone shrinks. In analogy with core saturation of regular geometries, the unsaturated zone disappears when R exceeds a certain threshold R_c and the shell is saturated throughout. A reasonably accurate estimate for the radius R_c can be obtained by setting the argument of the logarithm in Eq. 26 to unity, yielding

$$\kappa_0 R_c \simeq 3.5\gamma^{1/2} x_i (1 - x_i^2)^{-1/4}. \quad (31)$$

Complete saturation requires dimensions that greatly exceed typical sizes of astronomical masers, thus it is mostly only of theoretical interest.

5. Discussion

A shell becomes a sphere when $x_i \rightarrow 0$. Some of the expressions we list are based on the shell condition and diverge in that limit. These divergences can be avoided by employing the full expression for the unsaturated beaming angle (Eq. 12) instead of its shell limit (Eq. 10). The results display explicitly the transition between the two geometries at the price of greater complexity.

While a frequency dependence was never indicated explicitly, it enters through the frequency variation of κ_0 , the unsaturated absorption coefficient. The full absorption coefficient, including saturation effects, used in this study was assumed to obey the standard form proposed by Goldreich & Kwan (1974). This implies that our results are valid around line center up to frequency shifts of at least two Doppler widths (Elitzur 1994), covering practically all cases of interest. A more significant limitation is that, as with all maser solutions available to date, the one presented here is valid only for quiescent material. Complete analytic solutions for masers with large velocity gradients do not yet exist for any geometry. While the impetus for this study comes from the SiO interferometry results which indicate ring-like structures, these observations also show that the maser emission comes from

many compact spots, each one characterized by a different Doppler velocity (Diamond et al. 1994, Miyoshi et al. 1994, Greenhill et al. 1995). Each feature may thus correspond to a clump, defined either by a local enhancement of the pump rate (reflecting a favorable combination of conditions such as density, abundance, temperature, etc.) or velocity coherence in a turbulent medium. In either case, the geometry relevant to the maser radiation is the local one of the individual features, perhaps best described by elongated structures. On the other hand, the significant amount of flux lost in VLBI measurements due to over-resolution indicates that about one half of the total maser emission is much more extended than the VLBI spots. It is also known from measurements with lower spatial resolution that the total emission spreads over a region comparable in size to the ring seen in VLBI data. Indeed, if the distribution of a component of the emission smoothly fills up such a ring, it would very probably not be detectable in the high resolution experiments. Such extended masers would be described by the solution presented here.

The absence of observational data on such possible extended emission prevents further discussion at this time. As is the case for the spherical geometry with which it is closely associated, the primary importance of the shell maser solution may be in the insight it offers to maser behavior rather than direct comparison with current observations.

Acknowledgements. We thank the referee, Dr. W.H. Kegel, for his careful reading of the manuscript and useful comments and suggestions, especially for pointing out the general expression for the beaming angle, Eq. 12. This work was begun during a visit to Centro Astronomico de Yebes by M.E. He would like to thank the Center for its hospitality and the NSF for its partial support through grant AST-9321847. V.B. acknowledges partial support by DGICYT through grant PB93-0048.

References

- Bujarrabal, V., 1994, A&A, 285, 953
- Diamond, P.J., et al., 1994, ApJ, 430, L61
- Elitzur, M., 1990a, ApJ, 363, 628
- Elitzur, M., 1990b, ApJ, 363, 638 (E90)
- Elitzur, M., 1994, ApJ 422, 751
- Elitzur, M., Hollenbach, D.J. & McKee, C.F., 1992, ApJ, 394, 221
- Elitzur, M., McKee C.F., & Hollenbach, D.J., 1991, ApJ, 367, 333
- Goldreich, P., & Keeley, D.A., 1972, ApJ 174, 517
- Goldreich, P., & Kwan, J., 1974, ApJ 190, 27
- Greenhill, L.J., Colomer, F., & Bester, M., 1995, ApJ, 449, 365
- Miyoshi, M., et al., 1994, Nature 371, 395
- Reid, M.J., & Menten, K.M., 1990, ApJ 360, L51
- Western, L.R., & Watson, W.D., 1983, ApJ 275, 195